CHARACTERIZATION OF THE PRECIPITATION IN Al-Li-Cu-Mg-(Mn, Zr) ALLOYS

Laury Davin[1], Alfred Cerezo[1], Nong Gao[2], Marco Starink[2]

[1]Department of Materials, University of Oxford, Parks Road, Oxford OX1 3PH, UK

[2]Materials Research Group, School of engineering Sciences, University of Southampton, Southampton SO17 1BJ, UK

Abstract

The 3D atom probe has been used to characterise the precipitates in two Li-containing 2xxx series aluminium alloys: Al-6Li-Cu-Mg-0.2Mn (Alloy A) and Al-6Li-Cu-Mg-0.03Zr (Alloy B). The alloys have been heat-treated at 150°C for a range of times varying from 6h to 24h. In Alloy A, the particles identified can be classified into two categories: those rich in Cu and Mg (similar to GPB zones and S' precipitates) and δ', spherical particles rich in Li. Clusters rich in Li, are observed in addition to these particles. The same phases are observable in the Alloy B, though the growth of the δ' phase precipitates is accompanied by the formation of a Zr-rich phase similar to β'.

Keywords

3D atom probe, Al-Li-Cu-Mg-Zr, δ', β', S', GPB zones

[1] Corresponding authors. Tel.:+44-1865-273-694; fax:+44-1865-273-789
  e-mail address: Laury.davin@materials.ox.ac.uk

Introduction

New methods of production used in the aerospace industry require the design of new alloys from the 2xxx series which have enhanced formability but still retain good mechanical properties. The addition of lithium to Al-Cu-Mg alloys has the double advantage of reducing their density and increasing their elastic modulus. A large amount of work has been done on Al-Cu-Mg alloys including those realised thanks to the atom probe [1, 2]. However there have been few studies of the lithium-containing alloys of the 2xxx series. This paper reports a preliminary study of the precipitation sequence in two Al-Li-Cu-Mg-(Zr) alloys during the early stages (6h to 24h) of their heat-treatment at 150ºC. In order to elucidate the chemistry of these fine precipitates, materials were analysed in the 3D atom probe.

For these kinds of pseudo-quaternary alloys, four precipitation sequences can be given [3]:

All Al-Li alloys: $\alpha_{ss} \rightarrow \delta'(Al_3Li) \rightarrow \delta (AlLi)$

Al-Li-Mg: $\alpha_{ss} \rightarrow \delta'(Al_3Li) \rightarrow Al_2MgLi$

Al-Li-Cu (high Li:Cu): $\alpha_{ss} \rightarrow T_1(Al_2CuLi)$

Al-Li-Cu-Mg: $\alpha_{ss} \rightarrow GPB$ zones $\rightarrow S' \rightarrow S(Al_2CuMg)$

The addition of Zr is used to retard recrystallisation and grain growth as well as improving toughness, stress corrosion resistance and quench sensitivity.

The addition of Li to an Al-Cu-Mg alloy reduces the Cu and Mg solubility and thus increases the amount of Cu/Mg rich phases such as S'. T_2 (Al_2CuLi_3) and β' (Al_3Zr) have also been found. The formation of T_2 is believed to be suppressed at low ageing time and temperature [4]. β', like δ', precipitates has an Ll_2 structure and a spherical morphology [5].

Experimental

The composition of the two alloys studied is given in Tab.1. Both alloys were solutionised at 513ºC and stretched by 2.5% before heat treatment at 150ºC for 6h, 12h and 24h. The atom probe specimens were prepared by the standard two-stage electropolishing method using a solution of 25% perchloric acid in 75% acetic acid and a solution of 2% perchloric acid in 98% butoxyethanol. Specimens were analysed in the ECoPoSAP (Energy compensated position sensitive atom probe) at Oxford [6]. Analyses were carried out at a specimen temperature of 27K with a pulse fraction of 20% and a pulse repetition rate of 1500 Hz. The voltage varied between 4.5 and 9.5kV depending on the analysis. It should be noted that artefact such as preferential evaporation can affect the measured compositions (bulk and precipitates). However the overall compositions measured agree reasonably well with the nominal alloy compositions (Tab.1) and are closer than previous works done on ternary alloys [7]. The major discrepancy is in the measured of Cu and Li concentrations. All data given in this paper have been corrected for these differences.

Results and discussion

Clusters

Clusters have been found at every ageing time, even in the presence of larger precipitates. However their analysis was performed only in regions containing no such large precipitates. The clusters were identified using the nearest neighbour's atom method [8] [9]. In this method, solute-rich regions are formed by connecting solute atoms (in our case Li, Cu and Mg), which lie within a fixed distance (d).

Other atoms within some distance L greater than or equal to d are taken to belong to the clusters. Finally, clusters containing less than a minimum number of solute atoms (N_{min}) are eliminated. The values of d and L were fixed to 0.4 nm and the value of N_{min} used was 10 atoms of Li, Cu and Mg. To fix these values a random distribution was simulated. In such distribution, no (or few) clusters are expected if the correct parameters are used. Values for L in the range 0.4 and 1.2 show no dramatic variation in the solute composition of these clusters. The cluster density in alloy A, as well as the average composition, is given in Tab.2 for three different ageing times. These values were calculated over two or three runs. Each run contains from three to fifteen clusters and each cluster contains between fifty and one hundred atoms (including Al atoms). Between 6h and 12h the cluster density seems to be stable. At later stages, the density decreases as the same time at the overall matrix solute content begins to decrease. The clustering could then slow down in favour of the growth of the larger precipitates. The size of the clusters, as estimated from the radii of gyration, is similar for the three times of ageing (Tab.2).

Cu/Mg rich phases

In addition to the clusters, Cu and Mg rich precipitates were observed. In the early stages these precipitates are only composed of few atomic layers (fig.1). For longer ageing time, plate-like precipitates with an increasing size have been observed (fig.2a). The prior stretching is believed to reduce the nucleation of GPB zones and enhance the precipitation of the S' phases [10, 11]. However it seems that, in this case, the thin plates observed after 6h are similar in morphology and size to the GPB zones observed in the pseudo-binary Al-Cu-Mg-Mn alloy [12]. The larger plate-

shaped precipitates, with a Cu:Mg ratio close to unity, are the main Cu-bearing phase found in these alloys and hence are believed to be S' phases in agreement with observation by TEM and DSC studies on Al-Li-Cu-Mg alloys [13].

The average composition and dimensions of GPB zones and S' precipitates are given in Tab.3. From the atom probe results, a significant amount of Al appears to be incorporated in the Cu/Mg rich phases. This excess of Al in small particles has already been reported by several authors [14, 15] and might be attributed to trajectory aberrations. However, significant trajectory aberrations are associated with differences in apparent atomic density between precipitates and matrix. We observe very little difference in density within images containing these precipitates, which suggests only limited trajectory aberrations are present. Another hypothesis is that high level in Al can be required to reduce the lattice misfit and the interfacial energy of the particle [14].

Surprisingly, the Li content inside both zones and precipitates remains at the bulk level (fig. 1b and 2b). The presence of Li in S phase has already been observed in alloys with a high Cu:Li ratio [16]. T_1 (Al_2CuLi) and T_2 (Al_6CuLi_3) with a possible substitution of Li by Mg [17] are other possible candidates. In the present case, the precipitation of T_1 is to be excluded as the ratio Li+Mg/Cu in the precipitates is between two and three and therefore closer to T_2 stoichiometry. Finally, Lawson-Jack has proposed the existence of a S* phase with a stoichiometry of $Al_2Cu(Mg_{1-x}Li_x)$ where $0<x<1$ with a similar X-ray diffraction pattern to that of the R phase (Al_5CuLi_3) [18]. However, in our case, the relative constancy of the lithium level could indicate that Li is in solid solution in the S' phase and GPB zones.

Precipitation of δ'

In alloy A, δ' precipitates have been observed after 12h (Fig. 3a) and 24h. They are not present after 6h but their density increases with time thereafter. The numerous precipitates are spherical with an average diameter of 4.5 nm after 12 hours. As it can be seen on the composition profile of Fig. 3(b), the lithium content varies progressively from the interfaces to the heart of the precipitates to reach a maximum of 30%. After 24h, their size increases to 6 nm in diameter and the interfaces become more abrupt.

TEM observations show a fine precipitation of δ' particles in Alloy B heat treated for 24h. However, these homogeneously nucleated δ' were only rarely observed in the atom probe due to their lower density than in alloy A. Instead, a composite particle was found in this alloy heat treated for 12h. Its core is enriched in Zr and Li surrounded by a discontinuous shell rich in Li (fig 4). For several years, the Zr-rich phase β' (Al_3Zr) has been considered as a privileged nucleation site for the Li-rich phase δ' (Al_3Li) [19]. Hence, the core of the observed precipitate could be taken to be β' phase and the shell to be δ'. However the Zr content, with an average of 11%, is far below the stoichiometric level of 25%. It is possible that the low measured Zr content is due to preferential evaporation. Nevertheless, since the specimen is not representative of the bulk, we cannot use the overall composition to test this and correct the composition as discussed previously.

The morphology of the duplex δ'/ β' has been observed as spherical in previous TEM studies [20]. A spherical shape is also observed on the atom map when the difference in atomic density between the fcc structure of the Al matrix and the simple cubic structure of the β' phase is taken into account as shown in fig 4(a). The depth scaling for this atom map has been based on the atomic density for β' in order to show the

correct morphology for the precipitate. This means that the scaling is not correct for the Al matrix or the δ' phase. Composition profiles for Zr and Li through the selection box shown in Fig. 4(a) box are given in Fig. 4(b)-(d). The scaling used in these profiles has attempted to take into account the different atomic densities of the β', δ' and matrix. However, it is not easy to get an exact scaling under these conditions and therefore the thickness of the fcc transition phases between the matrix and the Zr-rich core are likely to be overestimated. The Al composition throughout the precipitate varies from 62% to 82% with an average of 77% which agrees with $Al_3(Zr,Li)$ stoichiometry. Li is present throughout the precipitate but the maximum level (26%) is found at one of the interface between the Zr/Li-rich core and the matrix.

Relationship between δ' and S phases

In alloy A, heat treated for 12h, all the Cu/Mg rich precipitates observed appear independent of the δ' precipitates. In this same alloy heat treated for 24h, they have been found either completely separated (i.e. observed during different analyses), independent but near each other or associated to form composite precipitates. In the latter case, two spherical Li-rich particles are at each end of the plate-like shaped Cu/Mg rich particles (Fig. 5) forming a dumbbell shape. The compositions of these precipitates are found to be the same as when the precipitates are observed separately. It therefore appears that the strain field around S' precipitates can facilitate the nucleation of δ', however these can also form homogeneously throughout the alloy.

Conclusion

1-Li-rich clusters were found in the alloy ageing at 150ºC for 6h, 12h and 24h. The density of the clusters varied with time, stable between 6 and 12 hours and then decreasing as the matrix concentration in Li is reduced.

2-Cu/Mg rich particles believed to be GPB zones and S' phases were observed in both alloys. The GPB zones, formed of few layers, nucleate from the earliest stages. The S' phases nucleate after 12h. Their content in Cu and Mg differ from the stoichiometry Al_2CuMg as the Al content inside the precipitate stays high and they are not depleted of Li.

3-Spherical δ' precipitates nucleate after 12h of heat treatment at 150ºC. Their size increases after 24h. They were found nucleating homogeneously in both alloys. In alloy A they were also observed associated with S' phase. In alloy B, they also nucleate around a Zr-rich phase.

4- A Li and Zr rich precipitate similar to a β'/δ' composite precipitate was found in alloy B aged to 12 hours at 150ºC.

References

[1]   K. Hono, N. Sano, S.S. Babu, R. Okano and T. Sakurai. (1993) Acta Metall. and Mater. 41, 829-838.

[2]   K. Hono, T. Sakurai and I.J. Polmear. (1994) Scripta Metall. et Mater. 30, 695-700.

[3]   P.J. Gregson. (1995) in High performance materials in aerospace (H.M. Flower, ed.), pp. 64-71, Chapman and Hall, London.

[4]   K. Satya Prasad, A.K. Mukhopadhyay, A.A. Gokhale, D. Banerjee and D.B. Goel. (1994) Scripta Metall. et Mater. 30, 1299-1304.

[5]   K.S. Kumar, S.A. Brown and J.R. Pickens. (1996) Acta Mater. 44, 1899-1915.

[6]   A. Cerezo, T.J. Godfrey, J.M. Hyde, S.J. Sijbrandij and G.D.W. Smith. (1994) Appli. Surf. Sci. 76/77, 374-381.

[7]   A. Menand, T. Al-Kassab, S. Chamberland and J.M. Sarrau. (1988) J. Phys. C6- 353-C6-358.

[8]   M.K. Miller. (2000), pp. 159, Klumer Academic/Plenum Publishers, New York.

[9]   D. Vaumousse, A. Cerezo and P.J. Warren. (2003) Ultramicroscopy 95, 215-221.

[10]   J.M. Galbraith, M.H. Tosten and P.R. Howell. (1987) J. Mater. Sci. 22, 27-36.

[11]   S.L. Dong, J.F. Mao, D.Z. Yang, Y.X. Cui and L.T. Jiang. (2002) Mater. Sci. and Eng. A 327, 213-223.

[12]   G. Nong, L. Davin, S. Wang, M. Starink and A. Cerezo. (2002) in 8th ICAA, Cambridge.

[13]   M. Starink and P.J. Gregson. (1996) Mater. Sci. and Eng. A 211, 54-65.

[14]   M. Murayama, K. Hono, W.F. Miao and L. D.E. (2001) Metall. and Mater. Trans. A 32A, 239-246.

[15]   S.K. Maloney, K. Hono, I.J. Polmear and S.P. Ringer. (1999) Scripta Mater. 41, 1031-1038.

[16]   A.K. Mukhopadhyay and V.V. Rama Rao. (1999) Mater. Sci. and Eng. A 268, 8-14.

[17]   H.M. Flower and P.J. Gregson. (1987) Mater. Sci. and Tech. 3, 81-90.

[18]   S.G. Lawson-Jack, H.M. Flower and D.R.F. West. (1993) Mater. Sci. and Tech. 9, 562-571.

[19]   F.W. Gayle and B. Vandersande. (1989) Acta Metall. 37, 1033-1046.

[20]   N. Boukos,E. Rocofyllou and C. Papastaikoudis. (1998) Mater. Sci. and Eng. A2565, 280-288.

	Li	Cu	Mg	Mn	Zr	Al
Alloy A	5.03±0.45	0.79±0.19	1.15±0.1	0.22±0.22	0(0.0003)	remainder
	(5.98)	(0.93)	(1.02)	(0.2)		
Alloy B	5.18±0.38	0.88±0.06	1.07±0.02	0(0.005)	0.14±0.25	remainder
	(5.8)	(0.94)	(1.12)		(0.03)	

Tab. 1: Measured Composition (%at) of the two alloys studied and nominal composition between bracket

		6h	12h	24h
Cluster density per m^3		$9.3(\pm4.7) \times 10^{23}$	$9.1(\pm5.5) \times 10^{23}$	$3.9(\pm1.8) \times 10^{23}$
Radius of gyration		0.44±0.07	0.46±0.10	0.46±0.09
Average composition (at%)	Al	82.8±2.2	84.2±2.3	78.7±3.9
	Li	12±0.8	12±0.9	11.2±1.1
	Mg	2.4±0.4	1.9±0.3	3.8±0.6
	Cu	2.5±0.4	1.4±0.3	2.8±0.6

Tab. 2: Density in cluster and their average composition in Alloy A after variable ageing time. Errors in composition are calculated on the total number of atoms within the clusters found for each heat treatment time

		GPB zone	S' phase
Dimensions in nm		2x7.4x17.8	5x17x27
Composition (at%)	Al	86.9±0.9	81.5±0.9
	Li	6.2±0.6	6.9±0.8
	Mg	3.4±0.5	5.6±0.6
	Cu	3.5±0.6	6±0.8

Tab 3: Average dimensions and composition of the Cu-Mg rich precipitates. Errors are based on standard deviation of the overall composition
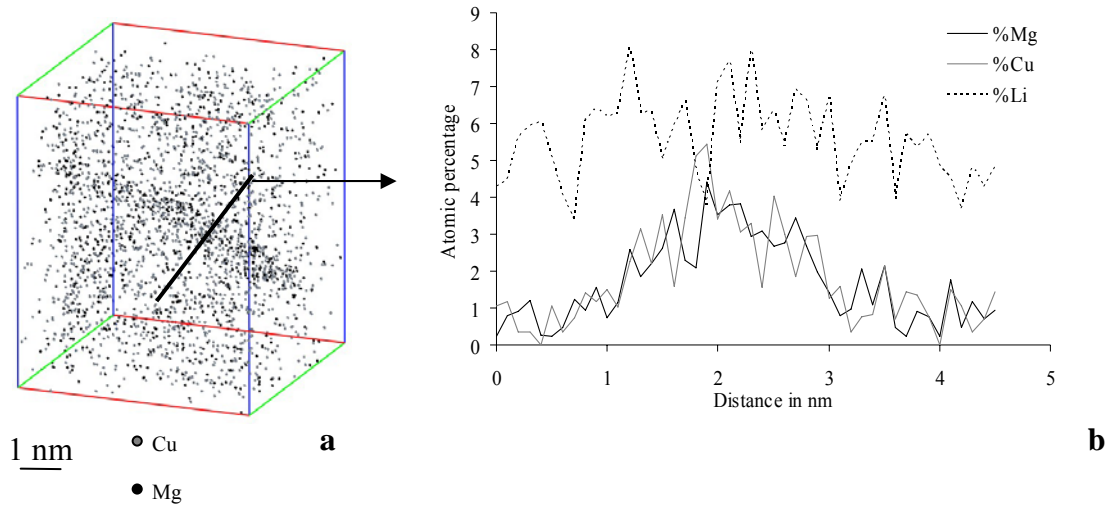
Fig 1: (a) 3DAP elemental mapping of Cu and Mg in Alloy A heat-treated at 150ºC for 6h showing a plate-like shape GPB zone (b) corresponding composition profile perpendicular to the zone/matrix broad interface
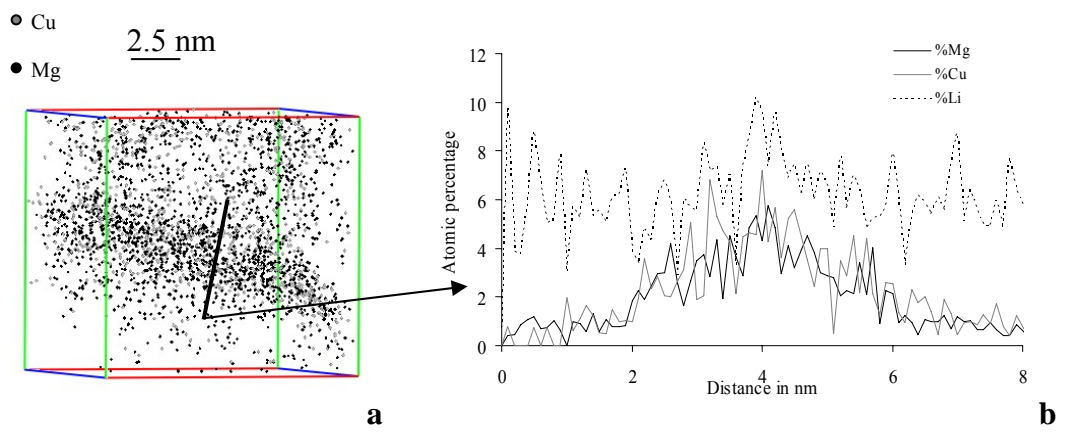

Fig 2: (a)3DAP elemental mapping of Cu and Mg in Alloy A heat-treated at 150ºC for 12h showing a plate-like shape S phase (b) corresponding composition profile perpendicular to the S'/matrix broad interface
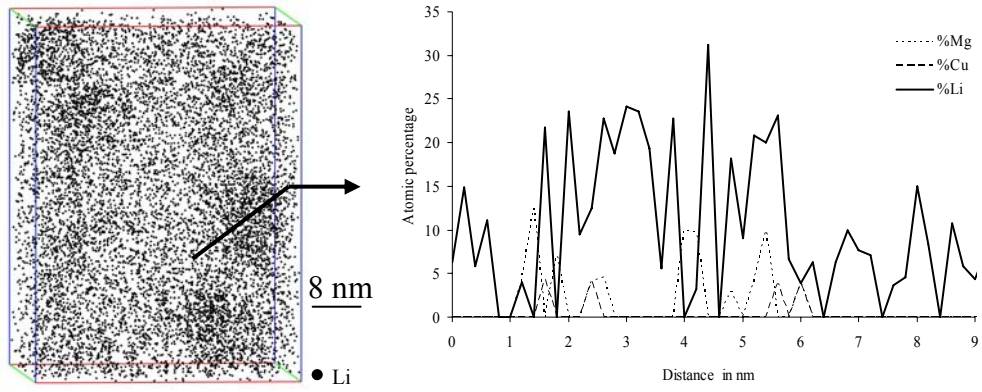
Fig 3: (a)3DAP elemental mapping of Li in Alloy A heat-treated at 150ºC for 12h exhibiting several δ' particles (b) composition profile through one of the δ' particles.
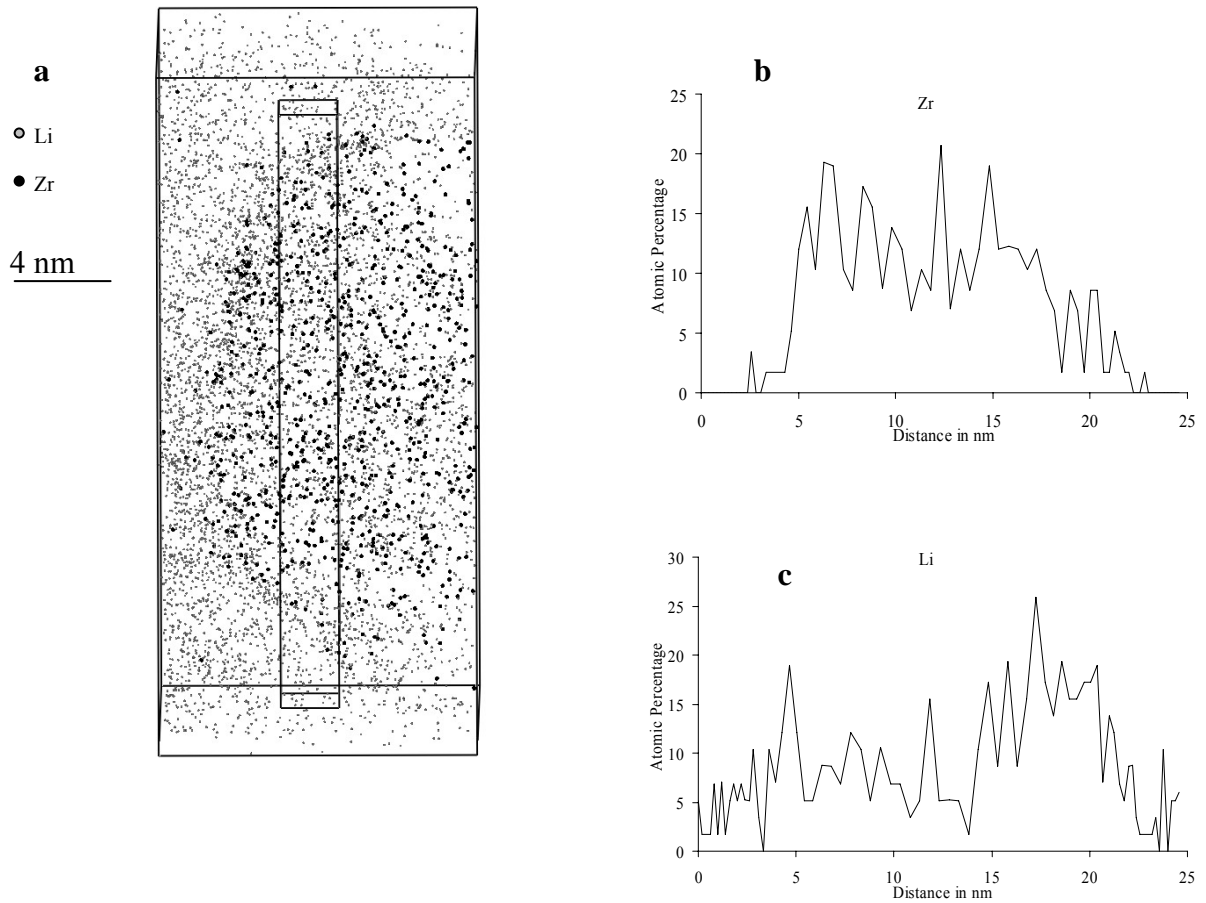
Fig 4: (a) 3DAP elemental mapping of Li and Zr in Alloy B heat-treated at 150ºC for 12h showing a spherical composite Zr/Li-rich precipitate. Li atoms are represented by grey spots and Zr atoms by black spots. Zr (b) and Li (c) composition profiles through the precipitate from the volume shown as a box in (a)
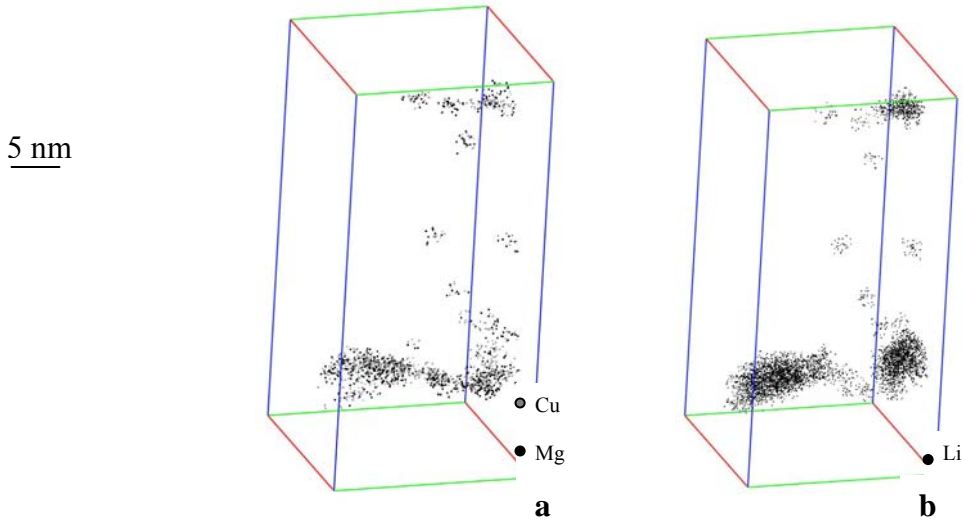

5 nm

Fig. 5: Composite precipitate with a S' precipitate (a) and two δ' particles (b) at each end.